Structural and magnetic properties of CoRh nanoparticles

E. O. Berlanga-Ramírez, F. Aguilera-Granja, and J. M. Montejano-Carrizales
Instituto de Física, Universidad Autónoma de San Luis Potosí, 78000 San Luis Potosí, Mexico

A. Díaz-Ortiz
Centro Nacional de Supercómputo, IPICyT, Apartato Postal 3-74 Tangamanga, 78231 San Luis Potosí, Mexico

K. Michaelian
Instituto de Física, Universidad Nacional Autónoma de México, 20-364, 01000 Distrito Federal, Mexico

A. Vega
Departamento de Física Teórica, Atómica, Molecular y Nuclear, Universidad de Valladolid, E-47011 Valladolid, Spain
(Received 6 January 2004; revised manuscript received 1 April 2004; published 13 July 2004)

The structural and magnetic properties of free-standing Co_nRh_m clusters ($N=n+m\approx 110$ and $n\approx m$) of three different symmetries—cubo-octahedral, icosahedral, and hcp—were investigated in two different chemical orders: segregated and alternated layering alloyed. The initial geometrical structures constructed at bulk distances were relaxed with a many-body Gupta potential to obtain the cluster geometries and energies. We find that the lowest energy in the different structures in all the cases corresponds to the segregated case (Rh-rich core surrounded by Co shells), and that the lowest energy is associated with the hcp structure. The interatomic distance for all the structures is slightly lower than the Rh bulk distance, in good agreement with the experimental observation , [Zitoun *et al.*, Phys. Rev. Lett. **89**, 037203 (2002)]. The spin-polarized electronic structure and related magnetic properties of these optimized geometries were calculated by solving self-consistently a *spd* tight-binding Hamiltonian. The magnetic moment of the Rh atoms shows a strong dependence on the position and environment, whereas the Co atoms show a smoother dependence. The magnetic moment of the Rh (Co) atoms in the alloying case are larger (lower) than the ones in the segregated case, however, the overall average for the segregated and alloying case are only slightly different for the different structures. The results are compared with the experimental data and with other theoretical calculations available in the literature.

DOI: 10.1103/PhysRevB.70.014410 PACS number(s): 75.75.+a, 36.40.Cg, 75.50.−y, 61.46.+w

I. INTRODUCTION

One of the most active research topics in condensed matter physics is the investigation of the finite-size effects in the magnetic properties of the 3*d* and 4*d* transition-metal (TM) systems like surfaces, superlattices, thin films, and clusters. It is well established that low dimensionality enhances the magnetic moments in the 3*d* ferromagnetic-TM clusters (Fe, Ni, and Co) and induces magnetic behavior in certain 4*d* TM systems like the ones composed of Rh, Ru, and Pd.[1–13] Another way to polarize these 4*d* TM elements is to create an intermetallic alloy with a ferromagnetic 3*d* TM.[14] In low-dimensional systems, it is expected that the superposition of the finite-size effects and the alloying with a ferromagnetic 3*d* TM leads to a particular magnetic behavior related to the interplay of both effects. In fact, such a phenomenon has been recently reported by Zitoun *et al.*[14] for CoRh nanoparticles of about 200 and 600 atoms synthesized experimentally. This is an example of a low-dimensional system investigated in this context. Most of the theoretical and experimental studies of the magnetic properties of CoRh systems have been performed on extended configurations like surfaces, superlattices, and sandwiches,[15–18] but not on clusters like those experimentally investigated by Zitoun *et al.*[14] Moreover, no other studies concerning the magnetic properties of binary clusters of the 3*d* and 4*d* elements have been reported in the literature so far for cluster sizes in the range of the experimental report. However, it is worth noticing that very recently some theoretical calculations using the density functional theory in the generalized gradient approximation (DFT-GGA) on the magnetic and structural properties have been done in the case of very small bimetallic clusters such as Co-Rh,[19] although the results are qualitatively consistent with experiments reported in the nanometric scale. However, it is still unclear at present to what extent this trend found in small clusters can be extrapolated to the nanometer size. In the case of surfaces, superlattices, and sandwiches, most of the works are oriented to the study of the giant antiferromagnetic coupling generated in the interface of the Co and Rh surfaces and its dependence with the distances and the spacer thickness for the superlattice like systems.[15–18] In the case of the Co-Rh clusters, the experiment has shown that the finite-size effects, together with the presence of the 3*d* ferromagnetic-TM, play a cooperative role that induces a magnetic moment in the rhodium atoms. This leads to a magnetism in the binary clusters of values comparable to or larger than that of the bulk alloy.[20,21]

It is well known that the geometrical structure plays an important role in the magnetism of clusters, and in the case of bimetallic clusters an additional ingredient comes from the chemical order. Therefore, for a correct understanding of the magnetic behavior of the bimetallic Co-Rh nanoparticles, it is relevant to investigate the local geometrical and chemical environments within the system in relation to the local

magnetic moment distribution. No clear experimental information on the structure and chemical order is yet available, although results[14] based on wide-angle x-ray scattering (WAXS) and radial distribution functions (RDF) suggest that the atomic distance in the clusters is approximately that of Rh bulk, that the structure may be icosahedral-like as reported for CoPt clusters,[22] and that segregation is not probable.

Sondón and Guevara[23] have studied the structural and magnetic properties of CoRh free-standing clusters of 13, 33, and 55 atoms using molecular dynamics with a Gupta potential for the structural part, and the tight-binding (TB) Hamiltonian for the electronic properties. They have found that the magnetic moment is not a linear function of the relative concentration of Co and Rh. For these cluster sizes, the lower-energy structures are icosahedral and they suggest a segregation of the cobalt atoms to the cluster surface. Such structures have also been found by other authors for pure Co, Rh, and other TM clusters of small sizes. In contrast, the phase diagram of the binary Co-Rh system shows that these metals form an hcp solid.[24] It is thus quite possible that a structural transition occurs for the Co-Rh clusters as the cluster size increases. The experiment of Zitoun *et al.*[14] concerns binary Co-Rh clusters larger than 55 atoms with relative Co and Rh concentrations close to 50%. It would be interesting to explore the competition between hcp, fcc, and icosahedral structures for Co-Rh clusters larger than 55 atoms, to investigate if the structure and local distribution of Co and Rh can modify the local magnetic properties of the system, and if this is reflected in the average magnetization, which is the experimentally accessible quantity. This is the aim of the present work.

To determine the role of the structure, bond size, and chemical order in the magnetic properties of bimetallic Co-Rh clusters of up to 115 atoms, we locally optimized some of the possible structures quoted by the experimentalists[14] such as icosahedral, fcc, and hcp structures with different chemical orders using a semiempirical Gupta potential for the different chemical orders. Although the problem of finding the true global minimum in bimetallic clusters of this size range is intractable due to the astronomical number of distinct permutations, and although the experiments of Zitoun *et al.* do not suggest crystalline structures, we assume that the three symmetries considered here, along with the two distinct chemical orders for each symmetry, provides a reasonable determination of role played by structure on the magnetic character of bimetallic Co-Rh. The actual geometries of these clusters will remain an open problem until more precise experimental data is available. For these relaxed structures we determined the electronic properties using a parametrized TB Hamiltonian in the mean-field approximation for *spd* valence electrons of Co and Rh. The same model has been used in our previous studies of small pure Co and Rh clusters.[6,11] In the following sections, we present the theoretical models and approximations used for the geometric and electronic parts of the problem. Next, we discuss the results and compare them with the experiment and available theoretical results. Finally, we present a summary and conclusions.

II. GEOMETRICAL MODEL AND APPROXIMATIONS

In this work, we have considered cluster sizes as large as possible ($N=n+m\approx 110$), which could be reasonably handled by the parametrized electronic calculation taking into account the large number of inequivalent sites generated in the different geometries and chemical orders investigated.

For the initial cluster geometries we assumed three different possible structures: (i) fcc truncated cubo-octahedral growth $N=111$, (ii) truncated icosahedral $N=115$, and (iii) hcp fragment $N=115$. The initial nearest-neighbor distance, in units of the Rh-bulk value (2.69 Å), between the atoms in the clusters was set equal to 1.0 for the fcc and the hcp, and to an average of 1.03 for the icosahedral due to the two types of interatomic distances within this cluster. In all cases, we fixed the composition as close as possible to the equiatomic concentration (Co_nRh_m with $n\approx m$) respecting symmetry of equivalent sites. Concerning the chemical order, we considered two possibilities: a segregated system and a homogeneous alloy. For the segregated case, we considered a Rh closed-shell core surrounded by Co layers. The homogeneous alloy was formed of Rh rich planes alternated with Co planes in a superlatticelike structure whose central plane is always a Rh plane (that is …Rh-Co-Rh-Co-Rh…). In this type of chemical order there is some amount of disorder due to the finite size of the cluster, particularly in the case of the icosahedral cluster (since this is not a crystalline fragment). The layer structure is similar to the $L1_0$ of the bulklike fcc for an equiatomic binary system. The geometrical shapes of the clusters used in this work facilitated the comparison of the effect of geometry on the magnetic character, since the systems are constructed of approximately the same number of atoms of both types for the different chemical orders (segregated and alloyed).

The cluster energies and optimized geometries were obtained by performing local conjugate gradient relaxations using an all atom, *n*-body Gupta potential modeling the interatomic interactions (see Refs. 6, 11, and 25 for details). The parameters of the potential for the interaction between atoms of the same metal were taken from the work of Cleri and Rosato[26] obtained from fits to the bulk lattice parameters and elastic constants. For the bimetallic (Co-Rh) interaction, we assumed an arithmetic mean of the individual radii parameters and a geometric mean of the potential depths. The local optimizations respected the geometric order, chemical order, and composition without the need of special precautions. On average, nearest-neighbor distances decreased by 2% from the nearest-neighbor distances of the bulk for the interior atoms, and by 2.5% for the surface atoms. The geometrical shapes of the clusters resulting from the optimization are illustrated in Fig. 1. The cobalt concentration x_{Co} and the binding energies per atom in eV of the locally optimized structures are also shown.

III. ELECTRONIC MODEL AND APPROXIMATIONS

Using the cluster geometries and interatomic distances obtained as described above, we calculated the magnetic-moment distribution of the clusters by self-consistently solv-

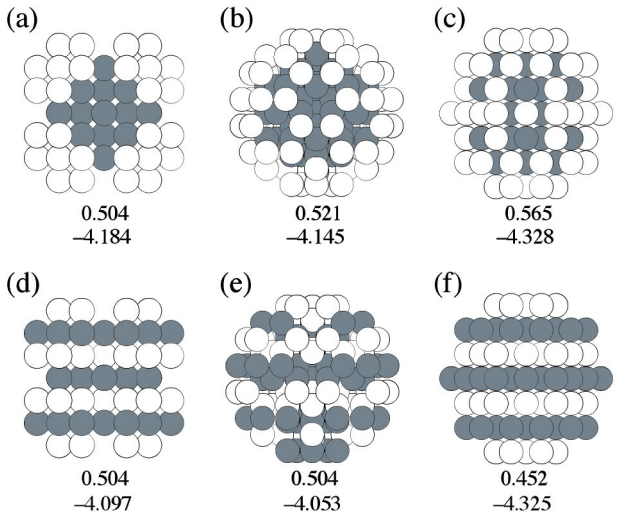

FIG. 1. Illustration of the cluster geometries obtained from the local optimization, where the white spheres represent the cobalt atoms and the gray ones correspond to rhodium atoms. The upper row corresponds to the segregated order and the lower one corresponds to the alloyed case. The three types of different structures are: (a) and (d) cubo-octahedral clusters $N=111$, (b) and (e) icosahedral clusters $N=115$, and (c) and (f) hexagonal close-packing cluster $N=115$. The cobalt concentration and the cohesive energy per atom in eV are given below each cluster respectively.

ing a TB Hamiltonian for the *s*, *p*, and *d* valence electrons in a mean-field approximation. In the usual second-quantization notation, the real space Hamiltonian H is given by

$$H = \sum_{i,\alpha,\sigma} \epsilon_{i\alpha\sigma} N_{i\alpha\sigma} + \sum_{\substack{i,\alpha,\sigma \\ i\neq j}} t_{ij}^{\alpha\beta} c_{i\alpha\sigma}^{\dagger} c_{j\beta\sigma}, \tag{1}$$

where $c_{i\alpha\sigma}^{\dagger}$ ($c_{j\beta\sigma}$) is the operator for the creation (annihilation) of an electron with spin σ and orbital state α (β) at atomic site i (j), and $N_{i\alpha\sigma}$ is the number operator. Electron delocalization within the system is described by the hopping integrals $t_{ij}^{\alpha\beta}$, which were included up to the second-nearest neighbors and assumed to be spin-independent. The hopping integrals between atoms of the same element were determined using the Slater-Koster approximation, with two-center hopping integrals reproducing the band structure of the bulk metal.[27] Since the interatomic distances in the clusters differed a little from the distances in the bulk, we assumed that in the neighborhood of the ideal first- and second-nearest-neighbors distances the hopping integrals obey the usual power law $(r_0/r_{ij})^{l+l'+1}$, where r_0 is the bulk first- (or second-) nearest-neighbor distance and l and l' are the orbital angular momenta of the spin-orbital states involved in the hopping process.[28] The heteronuclear hoppings were calculated as the geometrical average of the corresponding homonuclear hoppings, except for the two-center $pp\pi$ parameter between second neighbors, for which we use the arithmetic average because the Papaconstantopoulos' parameterization[27] produces a different sign in the case of Co and Rh.

The spin-dependent diagonal terms $\epsilon_{i\alpha\sigma}$ in the Hamiltonian include electron-electron interaction through a correction of the energy levels, and are given by

$$\epsilon_{i\alpha\sigma} = \epsilon_{i\alpha}^{0} + z_{\sigma} \sum_{\beta} \frac{J_{i,\alpha\beta}}{2} \mu_{i\beta} + \Omega_{i\alpha}. \tag{2}$$

Here, $\epsilon_{i\alpha}^{0}$ is the bare energy of orbital α at site i (that is, excluding Coulomb interactions). The second term is the correction for spin polarization of the electrons at site i ($\mu_{i\beta} = \langle N_{i\beta\uparrow}\rangle - \langle N_{i\beta\downarrow}\rangle$), that is, the local magnetic moment excluding the orbital part. In this second term, the $J_{i,\alpha\beta}$ are the exchange integrals and z_{σ} is the sign function ($z_{\uparrow}=+1; z_{\downarrow}=-1$). As usual, we have neglected the exchange integrals involving *sp* electrons, taking into account only the integral corresponding to the *d* electrons. Note that spin polarization of the delocalized *sp* band is also possible as a consequence of hybridization with the *d* states. As in our previous work on pure Co clusters,[6] the exchange integral of Co $J_{dd}(\mathrm{Co}) = 1.44$ eV was optimized in order to reproduce the bulk magnetic moment (without orbital contribution) of fcc cobalt $\overline{\mu} = 1.59\ \mu_{\mathrm{B}}$.[29] Since rhodium bulk is paramagnetic, we have optimized $J_{dd}(\mathrm{Rh}) = 0.40$ eV so that it provides simultaneously the best fit to the magnetic moments of the Rh_{13} and Rh_{19} clusters as calculated by Jinlong *et al.*[12] through the DFT method within the local spin-density approximation. This value of $J_{dd}(\mathrm{Rh})$ was used in our previous work on pure Rh clusters.[11] For Rh_{13} we obtained the same value as Jinlong *et al.*, whereas for Rh_{19} we slightly underestimated the magnetic moment; this value of $J_{dd}(\mathrm{Rh})$ corresponds to the best simultaneous fitting considering the dependence shown in Fig. 1 of Ref. 11. Those Rh-cluster sizes have been selected for the fit because the icosahedral and double icosahedral geometries are typical in almost all calculations. Finally, the site-and orbital-dependent self-consistent potential $\Omega_{i\alpha}$ assures the local electronic occupation, fixed in our model by doing a linear interpolation between the electronic occupations of the isolated atom and the bulk according to the actual local number of neighbors at the site *i*. For the isolated atoms we have taken the ground-state electronic occupations (7 *d* electrons and 2 *s* electrons for Co; 8 *d* electrons and 1 *s* electrons for Rh), whereas the electronic occupations for the corresponding bulk materials are those given by Papaconstantopoulos,[27] which are consistent with a first-principles scalar relativistic augmented plane-wave method (8.02 *d* electrons, 0.64 *s* electrons, and 0.34 *p* electrons for Co; 7.99 *d* electrons, 0.60 *s* electrons, and 0.41 *p* electrons for Rh). The local coordinations for the isolated atom and an atom in the fcc bulk are 0 and 12.6, respectively, provided that we consider a weight of 10% for the second neighbors relative to the first neighbors.

The spin-dependent local electronic occupations are self-consistently determined from the local densities of states

$$\langle \hat{n}_{i\alpha\sigma} \rangle = \int_{-\infty}^{\varepsilon_F} \mathcal{D}_{i\alpha\sigma}(\varepsilon) d\varepsilon, \tag{3}$$

which are calculated at each iteration by using the recursion method.[28] In this way, the distribution of the local magnetic

TABLE I. The relaxed interatomic bond distance and the number of first nearest-neighbors bonds for each type of the different possible atomic pairs. Interatomic bond distances are in units of the Rh-Rh bulk distance (2.69 Å).

		Segregated							
	N	Rh-Rh		Co-Co		Rh-Co		Average	
Cubo	111	0.992	234	0.981	90	0.983	120	0.987	444
Ico	115	0.994	216	1.016	96	0.970	120	0.992	432
hcp	115	0.993	186	0.986	123	0.991	192	0.991	501
		Alloy							
	N	Rh-Rh		Co-Co		Rh-Co		Average	
Cubo	111	0.987	86	0.984	96	0.989	262	0.987	444
Ico	115	0.986	80	0.978	64	0.993	288	0.988	432
hcp	115	0.990	141	0.992	108	0.992	252	0.991	501

moments ($\mu_i = \Sigma_\alpha \mu_{i\alpha}$) and the average magnetic moment per atom ($\overline{\mu} = (1/N)\Sigma_i \mu_i$) of the clusters are obtained at the end of the self-consistent cycle.

The description of the magnetic properties of low-dimensional 4*d* transition-metal systems requires the same ingredients as for the 3*d* series, in particular, the explicit consideration of the electronic delocalization in order to account for the itinerant character of the magnetism of these materials and also the symmetry of each system which plays an important role due to the directional bonding. The fact that this tight-binding model has been successfully applied to the study of pure Co and Rh clusters give us confidence in its utilization for the mixed clusters.

IV. RESULTS AND DISCUSSION

We first discuss the details of the optimized geometrical structures. In Fig. 1 we present a view of the investigated clusters. We assume three different possible structures: (i) cubo-octahedral growth (fcc) $N=111$, (ii) icosahedral $N=115$, and (iii) hcp $N=115$, and two different chemical orders: segregated and alloyed clusters. Notice that in the segregated clusters all surface atoms are of Co, and the slight disorder present in the case of the alloyed icosahedral cluster is due to the finite size and the noncrystalline structure. In Table I, we present the results of the relaxation for the different chemical orders and cluster geometries illustrated in Fig. 1. The initial nearest-neighbor (NN) distance was that of Rh bulk for the cubo-octahedral and hcp cases, whereas for the icosahedral case it was 1.03 times the Rh bulk distance. The results show a nontrivial relaxation in the atomic bonds as can be seen in the left-hand side of the first three columns of Table I. The average contraction within the cluster, regardless of the chemical species, is shown in the left-hand side of the fourth column. In general, the average bond length shrinks with respect to the Rh bulk value (taken as the unit), as expected, due to the finite size of the system.[6,11] The largest shrinking is presented for the icosahedral shape (≈3%), followed by the cubo-octahedral (≈1.5%), and finally the hcp (≈1%). These small compressions are reasonable con-

TABLE II. The average magnetic moments $\overline{\mu_i}$ per shell i, for clusters with segregation. A_i is the type of atom in the shell i and (Z_{Rh}, Z_{Co}) is the number of Rh and Co neighbors for A_i. The shells are ordered by increasing distance to the center of the clusters.

	Cubo-octahedron				Icosahedron				hcp			
i	A_i	N_i	$\overline{\mu_i}$	(Z_{Rh}, Z_{Co})	A_i	N_i	$\overline{\mu_i}$	(Z_{Rh}, Z_{Co})	A_i	N_i	$\overline{\mu_i}$	(Z_{Rh}, Z_{Co})
1	Rh	1	−0.11	(12,0)	Rh	1	−0.19	(12,0)	Rh	3	−0.15	(12,0)
2	Rh	12	0.04	(12,0)	Rh	12	−0.21	(12,0)	Rh	2	−0.17	(12,0)
3	Rh	6	0.18	(8,0)	Rh	30	0.23	(8,2)	Rh	3	−0.15	(10,2)
4	Rh	24	0.33	(7,3)	Rh	12	0.55	(6,5)	Rh	12	0.17	(10,2)
5	Rh	12	0.46	(5,4)	Co	60	2.45	(2,3)	Rh	6	0.22	(7,5)
6	Co	8	2.05	(3,6)					Rh	6	0.23	(7,5)
7	Co	48	2.50	(2,3)					Rh	6	0.67	(4,6)
8									Rh	6	0.97	(4,5)
9									Rh	6	0.62	(5,6)
10									Co	6	2.14	(4,4)
11									Co	12	2.15	(4,4)
12									Co	12	2.13	(4,4)
13									Co	3	2.38	(4,2)
14									Co	2	2.03	(3,6)
15									Co	6	2.48	(1,4)
16									Co	12	2.40	(2,4)
17									Co	12	2.44	(2,3)

sidering that previous semiempirical global optimization for pure Rh and Co clusters indicate that the interatomic distances reach the bulk values for relative small sizes.[6,11] On the right-hand side of the first four columns in Table I, we give the neighbor map, that is, the different numbers of the first NN pairs (FNNP), which provides insight on the geometrical order within the system. The total number of bondings are given in the right-hand side of the fourth column. In the segregated case approximately 50% of the FNNP are Rh-Rh, whereas in the alloy configuration 60% of the FNNP are Rh-Co. Therefore, one would expect the alloy configuration to display more pronounced 3*d*-4*d* cooperative effects than the segregated case. In our model the hcp structure is the one with the lowest energy (see Fig. 1), followed by the cubo-octahedral and the icosahedral. Concerning the chemical order, the lowest energy of the different structures corresponds to the segregated case, although for the hcp structure the cohesive energy is practically the same for both cases, i.e., for the segregated and alloyed cases. Notice, however, that the concentration for all the structures and chemical orders considered here is in general different and, therefore, a direct comparison among all the structures is valid only if the cohesive energy does not depend strongly on the relative concentrations of Co and Rh at values around 0.5. It is important to note that the experiment of Zitoun *et al.*[14] suggested that the lowest energy structure may be the icosahedral with a uniform Co-Rh distribution. It is pertinent now to analyze the influence of the chemical order and structure on the magnetic properties of the clusters.

In Tables II and III, we show the magnetic moments for the different structures and chemical orders for our optimized clusters as a function of the position and chemical environment. In Table II we give, for the segregated clusters [as illustrated in Figs. 1(a)–1(c)], the local magnetic moment μ_i of the different equivalent sites corresponding to the different shells (together with their multiplicity N_i). The coordination numbers Z_{Rh} and Z_{Co} are also given to identify the position of the atoms and the type of first NN's within the cluster, that is, the local chemical environment. We first analyze the particular chemical environment of the segregated clusters. In the case of the cubo-octahedral $N=111$, the inner Rh atoms form a 55 cubo-octahedral core and the surface Co atoms are located at the eight hexagonal umbrellalike spots (made of seven atoms) on the eight triangular faces of the 55 cubo-octahedral cluster. The number of Co surface atoms is 56 and the total number of atoms is 111. For the truncated icosahedral $N=115$, the inner Rh atoms form a complete icosahedral structure of 55 atoms, whereas the surface Co atoms are placed in a fullerene C-60-like surface whose sites belong to the surface of the 147 icosahedral cluster. In this way, we have 55 Rh-core atoms and 60 Co-surface atoms. In the hcp $N=115$, the inner Rh atoms are placed in five parallel planes of a total of 50 atoms surrounded by 65 Co atoms placed in seven parallel planes, all sites belonging to an hcp growth pattern.

From Table II, we can clearly see that for the segregated case, the central Rh atoms are antiferromagnetically aligned with the outer Rh atoms. The largest magnetic moment within the Rh core is obtained at the interface with Co, where a ferromagnetic Rh-Co alignment is also obtained.

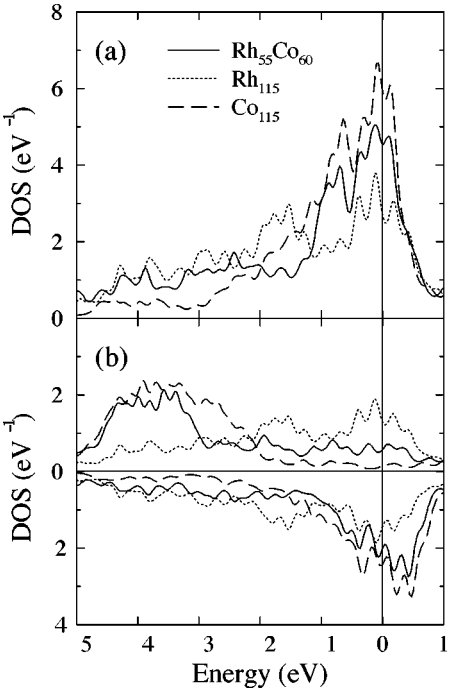

FIG. 2. The electronic density of states for three icosahedral clusters: segregated $Rh_{55}Co_{60}$, pure rhodium Rh_{115}, and pure cobalt Co_{115}. The upper panel (a) corresponds to the paramagnetic DOS, and the lower panel (b) corresponds to the magnetic DOS.

These trends are in agreement with the experimental results for Rh-Co superlattices and sandwiches, where at the interface, the Rh and Co atoms are ferromagnetically coupled (with a Rh magnetic moment of about 0.5 μ_B) and, at the same time, antiferromagnetic interactions occur in Rh far from the interface.[15,17,18] In our cluster geometries, the magnetic moments of the Rh atoms at the Rh-Co interface are in the range of 0.2 to 1.0 μ_B. In general, for the segregated configuration, the magnetic moment increases in moving away from the center of the cluster. At the interface, the larger number of Co atoms around a Rh site induces an enhancement of the magnetization in Rh sites. On the other hand, at the surface, the low coordination is associated with the high magnetic moment of the Co atoms. Both effects work in the same direction of increasing the magnetic moment of the cluster, which is otherwise slightly reduced due to the antiferromagnetic alignment at part of the Rh core. In order to understand the origin of the magnetic behavior of the Rh-Co clusters it is useful to analyze the electronic structure through both the paramagnetic and magnetic densities of electronic states. For this purpose, we have chosen, as an example, the icosahedral Rh-Co cluster of 115 atoms with the segregated configuration. In all the cases the Fermi level E_F is located at 0 eV. We compare the density of states (DOS) of this cluster with those corresponding to the pure Co_{115} cluster and the pure Rh_{115} cluster, both with the same icosahedral structure. In Fig. 2(a) we plot the total paramagnetic DOS per atom in the three clusters. One can clearly observe the larger peak at the Fermi level in the pure Co cluster which displays a narrower DOS. The DOS at E_F of the mixed cluster is between those of the pure clusters. The

TABLE III. The average magnetic moments $\overline{\mu_i}$ per shell i, for alloying clusters. A_i is the type of atom in the shell i and (Z_{Rh}, Z_{Co}) is the number of Rh and Co neighbors for A_i. The shells are ordered by increasing distance to the center of the clusters.

	Cubo-octahedron				Icosahedron				hcp			
i	A_i	N_i	$\overline{\mu_i}$	(Z_{Rh}, Z_{Co})	A_i	N_i	$\overline{\mu_i}$	(Z_{Rh}, Z_{Co})	A_i	N_i	$\overline{\mu_i}$	(Z_{Rh}, Z_{Co})
1	Rh	1	0.67	(4,8)	Rh	1	0.24	(6,6)	Rh	3	0.49	(6,6)
2	Rh	4	0.57	(4,8)	Rh	1	0.26	(6,6)	Co	2	1.66	(6,6)
3	Co	8	1.54	(8,4)	Rh	5	0.11	(6,6)	Rh	3	0.49	(6,6)
4	Rh	2	0.84	(4,4)	Co	1	1.39	(11,1)	Co	12	1.71	(6,6)
5	Rh	4	0.98	(2,6)	Co	5	1.40	(7,5)	Co	6	1.94	(6,6)
6	Rh	8	0.73	(4,6)	Rh	10	0.28	(4,6)	Rh	6	0.48	(6,6)
7	Co	16	1.80	(7,3)	Rh	5	0.18	(4,6)	Rh	6	0.52	(6,4)
8	Rh	4	1.02	(1,8)	Rh	5	0.34	(4,6)	Co	6	2.07	(5,4)
9	Rh	8	0.64	(4,5)	Co	5	1.84	(6,4)	Rh	6	0.44	(6,5)
10	Rh	8	0.81	(3,6)	Co	5	1.88	(6,4)	Rh	6	0.41	(4,4)
11	Co	16	2.49	(3,2)	Co	1	1.79	(11,0)	Co	12	2.18	(5,3)
12	Rh	16	1.01	(2,3)	Co	1	1.82	(5,6)	Rh	12	0.55	(4,4)
13	Co	16	2.64	(4,1)	Co	5	1.77	(5,6)	Rh	3	0.59	(4,2)
14					Co	5	1.78	(7,4)	Co	2	2.06	(3,6)
15					Rh	10	0.70	(2,3)	Rh	6	0.67	(3,2)
16					Rh	10	1.42	(1,4)	Rh	12	0.67	(3,2)
17					Rh	5	1.20	(1,4)	Co	12	2.40	(3,3)
18					Rh	5	0.54	(3,2)				
19					Co	10	2.51	(3,2)				
20					Co	10	2.51	(2,3)				
21					Co	5	2.49	(4,1)				
22					Co	5	2.46	(2,3)				

DOS of the pure Rh cluster is broader, consistent with the fact that the valence electrons of Rh are more external than those of Co.

Following the Stoner criterion one expects the pure Co cluster to have a stronger tendency to be magnetic than the mixed cluster, and the mixed cluster to have a stronger tendency than the pure Rh cluster. In the magnetic DOS of the three clusters [Fig. 2(b)], this trend is reflected in the splitting of the majority and minority states. The segregated cluster that we have chosen has a well-defined Rh-Co interface, thus allowing us to analyze separately the two parts. The DOS corresponding to the 55-atom Rh core and to the 60-atom Co cap can be compared with the corresponding parts of the pure Rh_{115} and pure Co_{115} clusters, respectively. This analysis allows a deeper insight into the hybridization effects and induction of spin polarization. In Figs. 3(a) and 3(b) we plot the paramagnetic and magnetic DOS of the Co cap of both the mixed and pure Co clusters. Notice that the surface effect clearly dominates over the Co-Rh hybridization. A narrow structure is present around E_F, which is similar in both clusters, indicating that little Rh character is present in the Co cap. The magnetic moment of these Co atoms in the pure cluster is only 0.01 μ_B larger than in the mixed cluster. These low-coordinated Co sites produce most of the magnetic character of the cluster. Comparing the paramagnetic DOS of the Rh core in the mixed cluster with that of the pure Rh cluster [Figs. 4(a) and 4(b)] one can notice that the Co-Rh hybridization effects are also small, only slightly larger than in the Co cap, and more precisely, slightly more important due to the fact that much less surface effect is present in the Rh sites. Then, from the Stoner criterion (see the paramagnetic DOS) one would expect a similar trend towards magnetism of the Rh atoms in both clusters. However, one must also take into account the external magnetic field that the Rh sites feel due to the surrounding Co atoms in the mixed cluster. This induces a noticeable spin polarization in the Rh core of the mixed cluster that contrasts with the nearly paramagnetic pure Rh_{115} cluster, with less than 0.1 μ_B in all atoms except the surface atoms which have 0.17 μ_B. From our analysis, we conclude that the presence of Co does not modify to any great extent the electronic structure of Rh through hybridization, but the high magnetic moment at the Co sites induces a noticeable spin polarization of the Rh atoms.

In Table III, we show the magnetic map obtained for the alloyed clusters [as illustrated in Figs. 1(d)–1(f)] in a similar way as that for the segregated clusters in Table II. Since in this case the geometrical description of the atoms is more difficult than in the segregated case, due to the alternate order of the two types of atoms, we limit by horizontal lines the inner core, the surface of the internal core, and the external surface atoms (see Table III). The inner core atoms have

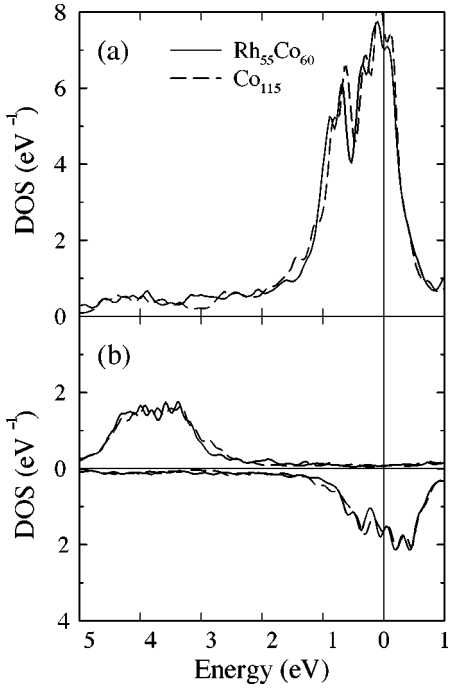

FIG. 3. The contribution of the electronic density of states of the outermost cobalt shell (C_{60} fullerenelike shell) of the icosahedral clusters $N=115$. The solid line corresponds to the case when the inner core is Rh_{55}, whereas the dashed line is for the case when the inner core is Co_{55}. The upper panel (a) corresponds to the paramagnetic DOS and the lower panel (b) corresponds to the magnetic DOS.

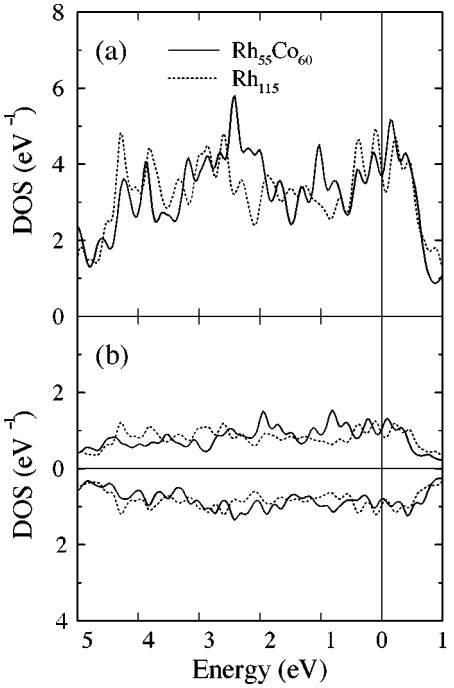

FIG. 4. The contribution of the electronic density of states of the icosahedral rhodium core Rh_{55} of the icosahedral clusters $N=115$. The solid line corresponds to the case when the external shell is Co_{60}, whereas the dotted line is for the case when the external shell is Rh. The upper panel (a) corresponds to the paramagnetic DOS and the lower panel (b) corresponds to the magnetic DOS.

coordination number 12, the atoms on the surface of the internal core have coordination numbers between 8 and 11, and the surface atoms in the cluster have coordination numbers equal to or smaller than 9. In contrast to the segregated case, for the alloyed case all the atoms are ferromagnetically coupled. The magnetic moments of the Rh atoms are, in general, larger than the ones of the segregated case due to the spin polarization induced by the Co atoms through hybridization. Furthermore, for the Rh atoms at the surface, even larger values of the magnetic moment are obtained, despite the fact of having, in some cases, less Co neighbors. This is due to the low-coordination effect that works in the same direction as the Co-Rh hybridization effect. For the Co atoms, the magnetic moments are smaller than the ones obtained in the segregated case due to the fact that now a larger hybridization with Rh is present (more Co-Rh nearest neighbors) as compared with the segregated situation.

An analysis of the local magnetic properties allows an understanding of the experimentally measurable average magnetic moments (AMM's). In Table IV, we show the AMM per Rh atoms ($\overline{\mu}_{Rh}$), per Co atoms ($\overline{\mu}_{Co}$), the AMM within the cluster ($\overline{\mu}$), the AMM per Rh-Co unit ($\overline{\mu}_{pair}=\overline{\mu}_{Rh}+\overline{\mu}_{Co}$), the Co concentration x_{Co}, and the ratio of the average Rh magnetic moment to the average Co magnetic moment $R=(\overline{\mu}_{Rh}/\overline{\mu}_{Co})$ for the different structures and chemical orders. The average magnetic moment of the Rh atoms in the segregated configuration is considerably smaller than in the alloyed case. For the Co atoms, instead, the opposite trend is found. Nevertheless, the overall average magnetic moment per atom is very similar for both chemical orders, the differences being in the order of the typical error bars in Stern-Gerlach experiments for pure Rh clusters.[30] The average magnetic moment per Rh-Co unit in the experiment is $\mu_{Rh\text{-}Co}=2.38\ \mu_B$, whereas our calculated values are 10% to

TABLE IV. The average values of the magnetic moments for the two components $\overline{\mu}_{Rh}$ and $\overline{\mu}_{Co}$ with the different chemical order and type of clusters, the average magnetic moment per Rh-Co unit $\overline{\mu}_{pair}$, the Co concentration x_{Co}, and the ratio of the average Rh magnetic moment to the average Co magnetic moment $R=(\overline{\mu}_{Rh}/\overline{\mu}_{Co})$.

	Segregated					
	$\overline{\mu}_{Rh}$	$\overline{\mu}_{Co}$	$\overline{\mu}$	$\overline{\mu}_{pair}$	x_{Co}	$\overline{\mu}_{Rh}/\overline{\mu}_{Co}$
Cubo	0.27	2.44	1.36	2.71	0.504	0.11
Ico	0.19	2.45	1.37	2.64	0.521	0.08
hcp	0.34	2.28	1.44	2.62	0.565	0.15
	Alloy					
	$\overline{\mu}_{Rh}$	$\overline{\mu}_{Co}$	$\overline{\mu}$	$\overline{\mu}_{pair}$	x_{Co}	$\overline{\mu}_{Rh}/\overline{\mu}_{Co}$
Cubo	0.84	2.20	1.53	3.04	0.504	0.38
Ico	0.64	2.13	1.39	2.77	0.504	0.30
hcp	0.55	2.06	1.23	2.61	0.452	0.27

30% higher. In previous theoretical calculations, Dennler *et al.*[19] reported a ratio R in the range of 0.43–0.53 within the framework of DFT-GGA for Co_2Rh_2 microclusters; Sondón and Guevara[23] using a tight-binding approximation, obtained $R \approx 0.6$ for a Rh-Co icosahedral cluster with 55 atoms; and finally in the bulk limit for a binary hcp Rh-Co system Moraitis *et al.*[20] obtained $R \approx 0.16$ using a tight binding linear muffin-tin orbital (TB-LMTO). Experimental investigations in Rh-Co thin-film alloys by Harp *et al.*[21] at room temperature give 0.25 for this ratio. In the present work this ratio for the segregated configuration goes from 0.08 to 0.15 (with an average value of 0.11), whereas for the alloyed case it goes from 0.27 to 0.38 (with an average value of 0.32), as given in the last column of Table IV. All the results for $R = (\overline{\mu}_{Rh}/\overline{\mu}_{Co})$ indicate that in general this ratio increases respect to the bulk value[20] when the size of the system is reduced.

The magnetic moments reported experimentally by Zitoun *et al.*[14] in Rh-Co clusters ($N=220$), assuming a homogeneous system and the bulk theoretical ratio of Moraitis *et al.*,[20] are $\mu_{Co}=2.02\ \mu_B$ and $\mu_{Rh}=0.32\ \mu_B$. Our calculation for smaller clusters ($N \approx 110$), give for the alloyed case a Co moment in the range of $2.06\ \mu_B - 2.20\ \mu_B$ and a Rh moment in the range of $0.55\ \mu_B - 0.84\ \mu_B$. For our most stable configuration, the hcp with segregation, we obtain $\mu_{Co}=2.28\ \mu_B$ and $\mu_{Rh}=0.34\ \mu_B$. Sondón and Guevara,[23] for the icosahedral cluster ($N=55$), give $2.02\ \mu_B$ for Co and $1.23\ \mu_B$ for Rh, respectively. Based on the previously discussed results, the bulk ratio μ_{Rh}/μ_{Co} used in the interpretation of the experimental results may not be adequate for these finite systems and in that case, the proposed experimental values would be slightly modified when a theory for finite-size system is used. Assuming an equiatomic homogeneous alloy with a superlatticelike structure like ours, and reinterpreting the experimental results of Zitoun *et al.*[14] in Rh-Co clusters ($N=220$) using the ratio calculated within our model ($\approx 1/3$), we would have for instance $\mu_{Co}=1.78\ \mu_B$ and $\mu_{Rh}=0.6\ \mu_B$. Interpretation of the experimental results should consider that this ratio depends on the system size. Moreover, this ratio also depends on the chemical order.

V. SUMMARY AND CONCLUSIONS

We studied the structural and magnetic properties of free-standing Co_nRh_m clusters ($N=n+m \approx 110$ and $n \approx m$) with three different symmetries: cubo-octahedral, icosahedral, and hcp, and with two different chemical orders: the segregated and the alternated layering alloyed. The optimization results indicate that the interatomic distance for all the structures is slightly lower (about 2%) than that of the Rh bulk distance, in good agreement with the experiment. We find that the lowest-energy chemical order corresponds to the segregated case, and that the lowest-energy structure is the hcp. However, for the hcp structure in particular, both chemical orders may coexist at room temperature due to the very small energy difference.

Since theoretical calculations[23] suggest that small RhCo clusters ($N \leqslant 55$) prefer the icosahedral structures, whereas bulklike systems form a hcp solid,[24] it is expected that a structural transition takes place at some intermediate size. From our calculations, this structural transition may be located at sizes in the range of hundreds of atoms. For all the clusters studied here the magnetic moment of the Rh atoms show a strong dependence on the geometrical and chemical environment. In particular, Rh atoms close to Co display a noticeable spin polarization induced by the magnetic moment of the surrounding Co atoms. This $3d$-$4d$ cooperative effect works in conjunction with the surface effect. The magnetic moment of the Rh (Co) atoms in the alloyed configuration are larger (smaller) than the ones in the segregated case; nevertheless, the average magnetic moment for a given structure is very similar in both chemical orders, with differences in the range of the typical experimental error bars for Rh clusters ($\pm 0.13\ \mu_B$).[30] Finally, from our results, as well as from other theoretical calculations,[19,20,23] it is found that the ratio $R=(\overline{\mu}_{Rh}/\overline{\mu}_{Co})$ depends on the size of the system as well as on the chemical order.

ACKNOWLEDGMENTS

This work was partially funded by CONACyT (Mexico) under Grant Nos. 39577-F, 40393-A, DGAPA-UNAM, and IN-104402. Financial support from the Spanish Ministry of Science and Technology (MCyT) Project No. MAT2002 04393 C02 01 and the Junta de Castilla-León Project No. VA 073/02 is gratefully acknowledged. F.A.-G. acknowledges PROMEP-SEP-CA230. Finally, E.O.B.-R. acknowledges CONACyT for financial support.

[1] W. A. de Heer, P. Milani, and A. Châtelain, Phys. Rev. Lett. **65**, 488 (1990).

[2] J. P. Bucher, D. C. Douglass, and L. A. Bloomfield, Phys. Rev. Lett. **66**, 3052 (1991).

[3] I. M. L. Billas, J. A. Becker, A. Châtelain, and W. A. de Heer, Phys. Rev. Lett. **71** 4067 (1993).

[4] I. M. Billas, A. Châtelain, and W. A. de Heer, Science **265**, 1682 (1994).

[5] F. Aguilera-Granja, S. Bouarab, M. J. López, A. Vega, J. M. Montejano-Carrizales, M. P. Iñiguez, and J. A. Alonso, Phys. Rev. B **57**, 12469 (1998).

[6] J. L. Rodríguez-López, F. Aguilera-Granja, K. Michaelian, and A. Vega, Phys. Rev. B **67**, 174413 (2003).

[7] A. N. Andriotis and M. Menon, Phys. Rev. B **59**, 15942 (1999).

[8] F. A. Reuse, S. N. Khanna, and S. Bernel, Phys. Rev. B **52**, 11650 (1995); F. A. Reuse and S. N. Khanna, Chem. Phys. Lett. **234**, 77 (1995).

[9] R. Guirado-López, D. Spanjaard, M. C. Desjonquĕres, and F. Aguilera-Granja, J. Magn. Magn. Mater. **186**, 214 (1998).

[10] J. Guevara, A. M. Llois, F. Aguilera-Granja, and J. M.

Montejano-Carrizales, Solid State Commun. **111**, 335 (1999).
[11] F. Aguilera-Granja, J. L. Rodríguez-López, K. Michaelian, E. O. Berlanga-Ramírez, and A. Vega, Phys. Rev. B **66**, 224410 (2002).
[12] Y. Jinlong, F. Toigo, and W. Kelin, Phys. Rev. B **50**, 7915 (1994).
[13] C. Barreteau, R. Guirado-López, D. Spanjaard, M. C. Desjonquéres, and A. M. Oles, Phys. Rev. B **61**, 7781 (2000).
[14] D. Zitoun, M. Respaud, M. C. Fromen, M. J. Casanove, P. Lecante, C. Amiens, and B. Chaudret, Phys. Rev. Lett. **89**, 037203 (2002).
[15] M. A. Tomaz, E. Mayo, D. Lederman, E. Hallin, T. K. Sham, W. L. O'Brien, and G. R. Harp, Phys. Rev. B **58**, 11493 (1998).
[16] D. C. A. Stoeffler, J. Magn. Magn. Mater. **165**, 62 (1997).
[17] S. Zoll, A. Dinia, M. Gester, D. Stoeffler, H. A. M. van der Berg, A. Herr, R. Poinsot, and H. Rakoto, J. Magn. Magn. Mater. **165**, 442 (1997).
[18] A. Rampe, D. Hartmann, W. Weber, S. Popovic, M. Reese, and G. Güntherodt, Phys. Rev. B **51**, 3230 (1995).
[19] S. Dennler, J. Morillo, and G. M. Pastor, Surf. Sci. **532-535**, 334 (2003); S. Dennler, J. L. Ricardo-Chavez, J. Morillo, and G. M. Pastor, Eur. Phys. J. D **24**, 237 (2003).
[20] G. Moraïtis, H. Dreysse, and M. A. Khan, Phys. Rev. B **54**, 7140 (1996).
[21] G. R. Harp, S. S. P. Parkin, W. L. O'Brien, and B. P. Tonner, Phys. Rev. B **51**, 12 037 (1995).
[22] T. Ould-Ely *et al.*, J. Phys. Chem. B **104**, 695 (2000).
[23] T. Sondón, M.Sc. Thesis, Comisión Nacional de Energía Atómica, 2003; and private communication with J. Guevara.
[24] W. Koster and E. Horn, Z. Metallkd. **43**, 444 (1952).
[25] K. Michaelian, N. Rendón, and I. L. Garzón, Phys. Rev. B **60**, 2000 (1999).
[26] F. Cleri and V. Rosato Phys. Rev. B **48**, 22 (1993).
[27] D. A. Papaconstantopoulos, *Handbook of the Band Structure of Elemental Solids* (Plenum, New York, 1986).
[28] R. Haydock, *Solid State Physics*, edited by E. Ehrenreich, F. Seitz, and D. Turnbull (Academic Press, London, 1980), Vol. 35, p. 215.
[29] C. Kittel, *Introduction to Solid State Physics*, 7th ed. (Wiley, New York, 1996).
[30] A. J. Cox, J. G. Louderback, and L. A. Bloomfield, Phys. Rev. Lett. **71**, 923 (1993); A. J. Cox, J. G. Louderback, S. E. Apsel, and L. A. Bloomfield, Phys. Rev. B **49**, 12 295 (1994).